J|A|C|S
COMMUNICATIONS

Published on Web 06/01/2007

Reversible Interconversion of Homochiral Triangular Macrocycles and Helical Coordination Polymers

Jungseok Heo, You-Moon Jeon, and Chad A. Mirkin*

Department of Chemistry and The International Institute for Nanotechnology, Northwestern University, 2145 Sheridan Road, Evanston, Illinois 60208-3113

Received March 9, 2007; E-mail: chadnano@northwestern.edu

Helical assemblies such as protein bundles and DNA are prevalent in biological systems and play key roles in molecular recognition, replication, and catalysis.[1] Several approaches have been developed for constructing abiological helices for potential applications in chiral separations, asymmetric catalysis, and nonlinear optics.[2−6] One promising approach is the use of coordination chemistry to direct the assembly of small component molecules into extended macromolecular helices. Related approaches have been used to prepare a wide variety of interesting molecular architectures such as triangles, squares, rectangles, prisms, and cages.[7−11] These approaches allow one to systematically design discrete and dispersible molecular systems as well as certain solid-state materials. One of the appealing aspects of this strategy is that, once a combination of building blocks and connecting units for preparing a desired structure have been identified, topological analogues can be obtained in many different sizes and with different functionalities through simple modifications of the building blocks. Herein, we report a novel synthetic strategy for preparing a triangular macrocyclic complex that can be spontaneously and reversibly transformed into a homochiral helical polymer simply through the addition of the appropriate solvent. The helicity of the homochiral polymer is dictated by the macrocycle enantiomer used to form it.

The chiral building block (*S*)-H_4**1** was designed to be a 60° corner in a molecular triangle **2** formed via metal coordination to its carboxylate groups (Scheme 1). To form such an angle, it is imperative that metal centers with *trans*-coordination sites be available for the assembly process.

(*S*)-H_4**1** was prepared in nearly quantitative yield by a one-step imine coupling reaction with the enantiopure (*S*)-binaphthyl diamine and 4-formyl-3-hydroxybenzoic acid. Interestingly, when (*S*)-H_4**1** and $Cu(OAc)_2 \cdot 6H_2O$ were reacted in a mixture of pyridine and methanol at room temperature, either cubic- or rod-shaped crystals were obtained, depending upon the solvent ratio. A 3:10 mixture of methanol and pyridine gave the dark green cubic crystals (path a), while a 10:1 mixture yielded similarly colored rod-shaped crystals (path b). In both cases, crystals suitable for single-crystal X-ray diffraction studies were obtained. The cubic crystals were indeed the targeted triangular structure **2**, and both enantiomers (*S*,*S*,*S*)-**2** and (*R*,*R*,*R*)-**2** have been structurally characterized (Figure 1). In the crystal structures of each enantiomer, a 3-fold symmetry axis passes through the center of the supramolecule forming three identical asymmetric units. The Cu···Cu distance between adjacent $\mathbf{1}^{Cu}$ centers is 16.77 Å, and the distance between connecting metal centers is 11.80 Å. The interconnecting Cu ions and $\mathbf{1}^{Cu}$ in (*S*,*S*,*S*)-**2** and (*R*,*R*,*R*)-**2** assume square pyramidal coordination geometries, and each of the axial positions on the Cu centers is occupied by a pyridine ligand. There are three small binding pockets in the molecular triangle, which are surrounded by four coordinating pyridine ligands and a salen unit (Figure 1b). Each hydrophobic pocket is occupied by a free pyridine molecule, and the three guest pyridine molecules assume a clockwise chiral arrangement within the macrocycle [(*R*,*R*,*R*)-**2** is shown as an example in Figure 1b].

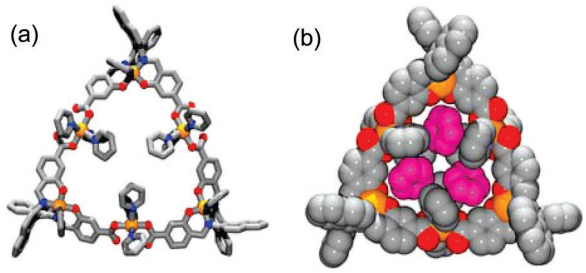

Figure 1. X-ray crystal structures of homochiral triangular complexes (a) (*S*,*S*,*S*)-**2** without guest pyridine molecules, (b) (*R*,*R*,*R*)-**2** including three pyridine guest molecules (pink) in the cavity. Hydrogen atoms are omitted for clarity.

Scheme 1. Solvent-Mediated Reversible Interconversion between the Triangular Macrocycle and the Helical Polymer (Inset: Coordination Environment of the Connecting Motif)[a]

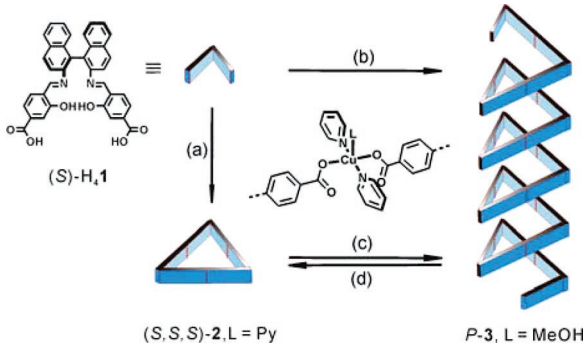

[a] Conditions: (a) $Cu(OAc)_2 \cdot 6H_2O$, MeOH/pyridine = 3/10; (b) $Cu(OAc)_2 \cdot 6H_2O$, MeOH/pyridine = 10/1; (c) MeOH; (d) pyridine.

Surprisingly, single-crystal X-ray analysis of one of the rod-shaped crystals shows that it is structurally related to compound **2** (Scheme 1), but rather than a molecular compound, it is a helical polymer **3**. One can see how polymer **3** can easily form from (*S*,*S*,*S*)-**2** by breaking one of the Cu−carboxylate interactions in (*S*,*S*,*S*)-**2** and twisting the structure slightly to re-form Cu−carboxylate interactions with additional equivalents of **2**. The enantiopure starting material (*S*)-H_4**1** results in the formation of a right-handed helical structure designated *P*-**3**. Interestingly, one not only can rationalize the formation of these two structures through this sequential bond breaking and reforming process but also realize it as a reversible chemical process.

The major difference between the connecting metal centers in these two structures is a weakly coordinating axial ligand to the Cu ion that interconnects the carboxylate groups on the periphery of the salen precursors. In the case of polymer **3**, the axial ligand is methanol, while in **2**, it is pyridine. This interconversion is a

10.1021/ja0716812 CCC: $37.00

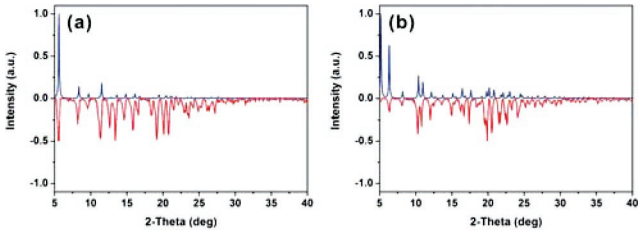

Figure 2. PXRD patterns: (a) **3** obtained from **2** by treatment of methanol, (b) **2** obtained from **3** by treatment of pyridine. Blue line, simulated from single-crystal structure; red line, PXRD pattern.

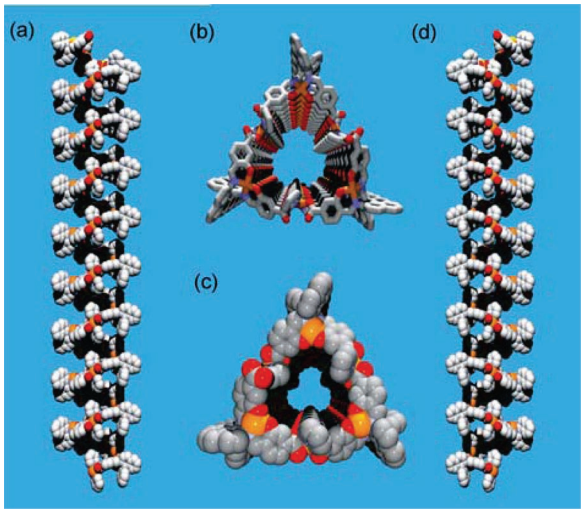

Figure 3. X-ray crystal structures of the helical polymers: (a, b) side view and top view of *P*-**3**, (c, d) top view and side view of *M*-**3**.

highly reversible process as evidenced by our ability to cycle between the molecular and polymeric structures five successive times. In addition, although the low solubility of the macrocycles and polymers made it difficult to analyze the conversion process in the solution state, the clean transformation between **2** and **3** could be easily followed and confirmed by powder X-ray diffraction (PXRD) by soaking the polymer in pyridine or the macrocycle in methanol (Figure 2).

The solid-state structure of *P*-**3** consists of a 1-D coordination polymer with a formula of $\{[Cu(Py_2,MeOH)\text{-}\mathbf{1}^{Cu}]\cdot 4MeOH\cdot 1.5H_2O\}_n$ (Figure 3). The asymmetric unit consists of a Cu^{2+} ion and a Cu salen moiety of which one carboxylate group coordinates to a second Cu^{2+} ion. This homochiral coordination polymer is helically folded and extended along the *c*-axis with a pitch of 14.3 Å, which is identical with the *c*-axis length of the unit cell. There are only right-handed *P*-helices in the crystals (it is a homochiral compound). In each helix, three $\mathbf{1}^{Cu}$ building blocks and three coordinating Cu ions constitute one turn. Each Cu ion is coordinated to two $\mathbf{1}^{Cu}$ building blocks in a linear fashion: $Cu-O_{avg} = 1.95$ Å, $O-Cu-O_{avg} = 177.5°$. The interconnecting Cu ions exhibit a square pyramidal coordination geometry with two equatorial pyridine ligands, two equatorial carboxylate ligands, and one axial methanol ligand.

The reason why *P*-**3** forms can be understood by analyzing its packing diagram. Each groove in the helix is intercalated by two other $\mathbf{1}^{Cu}$ units belonging to two adjacent helices generated by 3-fold screw symmetry operations along the *c*-axis (Supporting Information). This self-complementary packing stabilizes the helical structure and is possible only in the absence of an axial ligand on the $\mathbf{1}^{Cu}$ metal center. The helical channel inside the helical polymer is filled with solvent molecules (four methanol molecules and one and a half water molecules per repeat unit). These guest molecules are helically aligned along the channel-forming double-helix-like structure. The volume of solvent accessible voids is estimated to be 35% of the total volume in the crystal.

In conclusion, we have discovered an unusual solvent-induced transformation between a triangular macrocycle and a helical coordination polymer. The chirality of the ligand precursors dictates the helicity of the resulting polymer. In addition to providing an efficient synthetic route to topologically intriguing supramolecules, this work demonstrates the subtle interplay between two energetically similar molecular and polymer structures. One has to wonder why similar transformations have not been observed for dimers, squares, and other supramolecules prepared by the directional bonding approach. In all cases, one can make the analogous transformation through a simple intramolecular bond breaking, distortion, and intermolecular bond forming process. Efforts to explore the breadth and scope of this phenomenon are underway.

Acknowledgment. C.A.M. acknowledges NSF, ONR, ARO, DDRE, and AFOSR for support of this research. Portions of this work were performed at the DuPont−Northwestern−Dow Collaborative Access Team (DND-CAT) Synchrotron Research Center located at Sector 5 of the Advanced Photon Source. DND-CAT is supported by the E.I. DuPont de Nemours & Co., the Dow Chemical Company, the U.S. National Science Foundation through Grant DMR-9304725 and the State of Illinois through the Department of Commerce and the Board of Higher Education Grant IBHE HECA NWU 96.

Note Added after ASAP Publication. An error was corrected in the last sentence of paragraph six on June 1, 2007.

Supporting Information Available: Detailed experimental procedures and X-ray crystallographic data for (*S*,*S*,*S*)-**2** and (*R*,*R*,*R*)-**2**, *P*-**3**, and *M*-**3**. This material is available free of charge via the Internet at http://pubs.acs.org.

References

(1) Bell, T. W.; Jousselin, H. *Nature* **1994**, *367*, 441−444.
(2) (a) Barboiu, M.; Lehn, J.-M. *Proc. Natl. Acad. Sci. U.S.A.* **2002**, *99*, 5201−5206. (b) Ramírez, J.; Stadler, A.-M.; Kyritsakas, N.; Lehn, J.-M. *Chem. Commun*. **2007**, 237−239. (c) Baxter, P. N. W.; Khoury, R. G.; Lehn, J.-M.; Baum, G.; Fenske, D. *Chem.—Eur. J.* **2000**, *6*, 4140−4148.
(3) Cui, Y.; Lee, S. J.; Lin, W. *J. Am. Chem. Soc.* **2003**, *125*, 6014.
(4) Whang, D.; Heo, J.; Kim, C.-A.; Kim, K. *Chem. Commun.* **1997**, 2361−2362.
(5) Tabellion, F. M.; Seidel, S. R.; Arif, A. M.; Stang, P. J. *Angew. Chem., Int. Ed.* **2001**, *40*, 1529−1532.
(6) Pantoş, D. G.; Pengo, P.; Sanders, J. K. M. *Angew. Chem., Int. Ed.* **2007**, *46*, 194−197.
(7) (a) Farrell, J. R.; Mirkin, C. A.; Guzei, I. A.; Liable-Sands, L. M.; Rheingold, A. L. *Angew. Chem., Int. Ed.* **1998**, *37*, 465−467. (b) Holliday, B. J.; Mirkin, C. A. *Angew. Chem., Int. Ed.* **2001**, *40*, 2022−2043. (c) Gianneschi, N. C.; Masar, M. S., III; Mirkin, C. A. *Acc. Chem. Res.* **2005**, *38*, 825−837.
(8) Fiedler, D.; Leung, D. H.; Bergman, R. G.; Raymond, K. N. *J. Am. Chem. Soc.* **2004**, *126*, 3674−3675.
(9) Hiraoka, S.; Fujita, M. *J. Am. Chem. Soc.* **1999**, *121*, 10239−10240.
(10) Kitaura, R.; Onoyama, G.; Sakamoto, H.; Matsuda, R.; Noro, S.-i.; Kitagawa, S. *Angew. Chem., Int. Ed.* **2004**, *43*, 2684−2687.
(11) (a) Gianneschi, N. C.; Bertin, P. A.; Nguyen, S. T.; Mirkin, C. A.; Zakharov, L. N.; Rheingold, A. L. *J. Am. Chem. Soc.* **2003**, *125*, 10508−10509. (b) Gianneschi, N. C.; Cho, S.-H.; Nguyen, S. T.; Mirkin, C. A. *Angew. Chem., Int. Ed.* **2004**, *43*, 5503−5507.

JA0716812